

# Exemplar VAEs for Exemplar based Generation and Data Augmentation

Sajad Norouzi<sup>1</sup> David J. Fleet<sup>1</sup> Mohammad Norouzi<sup>2</sup>

## Abstract

This paper presents a framework for exemplar based generative modeling, featuring Exemplar VAEs. To generate a sample from the Exemplar VAE, one first draws a random exemplar from a training dataset, and then stochastically transforms that exemplar into a latent code, which is then used to generate a new observation. We show that the Exemplar VAE can be interpreted as a VAE with a mixture of Gaussians prior in the latent space, with Gaussian means defined by the latent encoding of the exemplars. To enable optimization and avoid overfitting, Exemplar VAE’s parameters are learned using leave-one-out and exemplar subsampling, where, for the generation of each data point, we build a prior based on a random subset of the remaining data points. To accelerate learning, which requires finding the exemplars that exert the greatest influence on the generation of each data point, we use approximate nearest neighbor search in the latent space, yielding a lower bound on the log marginal likelihood. Experiments demonstrate the effectiveness of Exemplar VAEs in density estimation, representation learning, and generative data augmentation for supervised learning. The code is available at <https://exemplar-vae.github.io>.

## 1. Introduction

Consider the problem of conditional image generation, given a natural language description of a scene such as

“A woman is staring at Monet’s Water Lilies”.

There are two general strategies for addressing this problem. One can resort to *exemplar based methods*, e.g., using web search engines to [retrieve photographs with similar captions](#), and then edit the retrieved images to generate new ones. Alternatively, one can adopt *parametric models* such as deep neural networks optimized for text to image translation to synthesize new relevant scenes.

<sup>1</sup>University of Toronto and Vector Institute <sup>2</sup>Google Research.  
Correspondence to: S. Norouzi <[sajadn@cs.toronto.edu](mailto:sajadn@cs.toronto.edu)>, D. Fleet <[fleet@cs.toronto.edu](mailto:fleet@cs.toronto.edu)>, M. Norouzi <[mnorouzi@google.com](mailto:mnorouzi@google.com)>.

This paper presents a machine learning framework for exemplar based generative models using expressive neural nets, combining the advantages of both exemplar based and parametric paradigms. Here we focus on simple unconditional generation tasks, but the learning formulation and the methods developed are generally applicable to many potential applications including text to image translation.

Exemplar based methods depend on large and diverse datasets of exemplars and relatively simple machine learning algorithms, such as Parzen window estimation (Parzen, 1962) and conditional random fields (Lafferty et al., 2001). They deliver impressive results on texture synthesis (Efros & Leung, 1999), image super resolution (Freeman et al., 2002), and inpaiting (Criminisi et al., 2003; Hays & Efros, 2007), despite their simplicity. These techniques can accommodate web scale datasets with a improvement in sample quality as the dataset size increases, without the need for further optimization of model parameters. The success of exemplar based methods hinges on the distance metric used to build a local density model for each neighborhood. Unfortunately, finding an effective distance metric in a high dimensional space is challenging on its own (Xing et al., 2003; Johnson et al., 2016). Further, while exemplar based methods excel in interpolation tasks, they often underperform their parametric counterparts in extrapolation.

Parametric generative models based on deep neural nets enable learning complex data distributions across myriad problem domains (e.g., Oord et al. (2016); Reed et al. (2016)). Predominant models, such as Variational Autoencoders (VAEs) (Kingma & Welling, 2014; Rezende et al., 2014), Normalizing Flows (Dinh et al., 2014; 2016), and Generative Adversarial Networks (GANs) (Goodfellow et al., 2014a), adopt a decoder network to convert samples from a prior distribution, often a factored Gaussian, into samples from the target distribution. After the completion of training, these models discard the training data and generate new samples using decoder networks alone. Hence, the burden of generative modeling rests entirely on the parametric model. Further, with the availability of additional training data, these models require re-training or fine-tuning.

This paper investigates a general framework for *exemplar based generative modeling* and a particular instantiation of this framework called the *Exemplar VAE*. To sample

from the Exemplar VAE, one first draws a random exemplar from a training dataset and then stochastically transforms that exemplar into a new observation. We are inspired by recent work on generative models augmented with external memory (*e.g.*, Guu et al. (2018); Li et al. (2019); Tomczak & Welling (2018); Khandelwal et al. (2019); Bornschein et al. (2017)), but unlike most existing work, we do not rely on a prespecified distance metric to define the neighborhood structure. Instead, we simultaneously learn a latent space and a distance metric suited for generative modeling.

Exemplar VAE can be interpreted as a VAE with a Gaussian mixture prior in the latent space, with one component per exemplar. The component means are defined by the latent encoding of the exemplars. We build on the VampPrior formulation of Tomczak & Welling (2018), and our work is a continuation of recent papers on enhancing VAEs with richer latent priors (Kunin et al., 2019; Bauer & Mnih, 2018; Lawson et al., 2019).

The main contributions of this paper include:

- The development of the Exemplar VAE and a framework for exemplar based generative modeling.
- The proposal of critical regularization methods, enhancing generalization of exemplar based generative models.
- The use of approximate nearest neighbor search to formulate a lower bound on ELBO to accelerate learning.

Our experiments demonstrate that Exemplar VAEs consistently outperform VAEs with a Guassian prior and a Vamp-Prior on density estimation and represenation learning. Further, unsupervised data augmentation using Exemplar VAEs proves to be extremely helpful, resulting in a classification error rate of 0.69% on permutation invariant MNIST.

## 2. Exemplar based Generative Models

We define an exemplar based generative model in terms of a dataset of  $N$  exemplars,  $X \equiv \{\mathbf{x}_n\}_{n=1}^N$ , and a parametric transition distribution,  $T_\theta(\mathbf{x} \mid \mathbf{x}')$ , which stochastically transforms an exemplar  $\mathbf{x}'$  into a new observation  $\mathbf{x}$ . The log density of a data point  $\mathbf{x}$  under an exemplar based generative model  $\{X, T_\theta\}$  is expressed as

$$\log p(\mathbf{x} \mid X, \theta) = \log \sum_{n=1}^N \frac{1}{N} T_\theta(\mathbf{x} \mid \mathbf{x}_n), \quad (1)$$

where we assume the prior probability of selecting each exemplar is uniform.

The transition distribution  $T_\theta(\mathbf{x} \mid \mathbf{x}')$  can be defined using any expressive parametric generative model, including VAEs, Normalizing Flow and auto-regressive models. Any reasonable transition distribution should put a considerable probability mass on the reconstruction of an exemplar from itself, *i.e.*,  $T_\theta(\mathbf{x} \mid \mathbf{x})$  should be large for all  $\mathbf{x}$ . Further, an ideal transition distribution should be able to model the conditional dependencies between different dimensions of

$\mathbf{x}$  given  $\mathbf{x}'$ , since the dependence of  $\mathbf{x}$  on  $\mathbf{x}'$  is often insufficient to make dimensions of  $\mathbf{x}$  conditionally independent.

One can think of Kernel Density Estimation (KDE), also known as Parzen window estimates (Parzen, 1962), as the simplest instance of exemplar based generative models, in which the transition distribution is defined in terms of a prespecified kernel function and its meta-parameters. For example, with a Gaussian kernel, KDE takes the form

$$\log p(\mathbf{x} \mid X, \sigma^2) = \log \sum_{n=1}^N \frac{1}{N} \exp \frac{-\|\mathbf{x} - \mathbf{x}_n\|^2}{2\sigma^2} - \log C, \quad (2)$$

where  $\log C = d_x \log(\sqrt{2\pi}\sigma)$  is the log normalizing constant for an isotropic Gaussian in  $d_x$  dimensions. The non-parametric nature of KDE enables one to exploit extremely large heterogeneous datasets of exemplars and apply nearest neighbor search techniques to density estimation. That said, simple KDEs underperform neural density estimation, especially in high dimensional spaces, due to the inflexibility of typical transition distributions, *e.g.*, when  $T(\mathbf{x} \mid \mathbf{x}') = \mathcal{N}(\mathbf{x} \mid \mathbf{x}', \sigma^2 I)$ .

This work aims to adopt desirable properties of non-parametric exemplar based models to help scale parametric models to large heterogeneous datasets.

### 2.1. Optimization

We use expressive parametric density functions to represent the transition distribution  $T_\theta(\mathbf{x} \mid \mathbf{x}')$  within an exemplar based framework (1). Consistent with recent work (Tomczak & Welling, 2018; Bornschein et al., 2017), we find that simply maximizing the expected log marginal likelihood over the empirical training data,

$$O(\theta; X) = \sum_{i=1}^N \log \sum_{n=1}^N \frac{1}{N} T_\theta(\mathbf{x}_i \mid \mathbf{x}_n), \quad (3)$$

to find the parameters of the transition distribution ( $\theta$ ) results in massive overfitting. This is not surprising, since a flexible transition distribution can put all its probability mass on the reconstruction of each exemplar, *i.e.*,  $p(\mathbf{x} \mid \mathbf{x})$ , yielding high log-likelihood on training data but poor generalization.

We propose two simple but effective *regularization* strategies to mitigate overfitting in exemplar based generative models:

1. **Leave-one-out during training.** The generation of a given data point is expressed in terms of all exemplars except that point. The non-parametric nature of the generative model enables easy adoption of such a leave-one-out (LOO) objective during training, to optimize

$$O_1(\theta; X) = \sum_{i=1}^N \log \sum_{n=1}^N \frac{\mathbb{1}_{[i \neq n]} T_\theta(\mathbf{x}_i \mid \mathbf{x}_n)}{N-1}, \quad (4)$$

where  $\mathbb{1}_{[i \neq n]} \in \{0, 1\}$  is an indicator function taking the value of 1 if and only if  $i \neq n$ .

2. **Exemplar subsampling during training.** In addition to LOO, we observe that explaining a training point using a subset of the remaining training exemplars improves generalization. To that end we use a hyper-parameter  $M$  to define the exemplar subset size for the generative model. To generate  $\mathbf{x}_i$  we draw  $M$  exemplar indices, denoted  $\pi \equiv \{\pi_m\}_{m=1}^M$ , uniformly at random from subsets of  $\{1, \dots, i-1, i+1, \dots, N\}$ . Let  $\pi \sim \Pi_M^{N,i}$  denote this sampling procedure with  $(N-1 \text{ choose } M)$  possible subset outcomes. Combining LOO and exemplar subsampling, the objective takes the form

$$O_2(\theta; X) = \sum_{i=1}^N \mathbb{E}_{\pi \sim \Pi_M^{N,i}} \log \sum_{m=1}^M \frac{1}{M} T_\theta(\mathbf{x}_i \mid \mathbf{x}_{\pi_m}). \quad (5)$$

Note that by moving  $\mathbb{E}_\pi$  inside the log in (5) we recover  $O_1$ ; *i.e.*, via Jensen's inequality,  $O_2$  is a lower bound on  $O_1$ . Nevertheless, even when training with  $O_1$  is possible, we find that  $O_2$  yields better generalization.

Once training is completed, we use all  $N$  training exemplars to explain the generation of validation or test points using (1). Hence, the regularization techniques discussed above (LOO and exemplar subsampling) are not relevant to inference. The non-parametric nature of an exemplar based model is compatible with such regularization techniques, the use of which is not straightforward for training parametric generative models. Even though cross validation is commonly used for parameter tuning and model selection, here cross validation is used as a training objective directly, suggestive of a *meta-learning* perspective.

Exemplar sub-sampling is also very similar to Dropout (Srivastava et al., 2014) where we drop some mixture components in the latent space during training to encourage better generalization at the test time. Like conventional dropout, we still use the complete model for evaluation.

### 3. Exemplar Variational Autoencoders

We present the *Exemplar VAE* as an instance of neural exemplar based generative models, in which the transition distribution  $T(\mathbf{x} \mid \mathbf{x}')$  is defined in terms of the encoder  $\tilde{q}_\phi$  and the decoder  $p_\theta$  of a VAE, *i.e.*,

$$T(\mathbf{x} \mid \mathbf{x}') = \int_z \tilde{q}_\phi(\mathbf{z} \mid \mathbf{x}') p_\theta(\mathbf{x} \mid \mathbf{z}) d\mathbf{z}. \quad (6)$$

The Exemplar VAE assumes that, given  $\mathbf{z}$ , an observation  $\mathbf{x}$  is conditionally independent from the associated exemplar  $\mathbf{x}'$ . This conditional independence assumption helps simplify the formulation, enabling efficient optimization.

The generative process of an Exemplar VAE has three steps:

1. Sample  $n \sim \text{Uniform}(1, N)$  to draw a random exemplar  $\mathbf{x}_n$  from the training set  $\{\mathbf{x}_n\}_{n=1}^N$ .
2. Sample  $\mathbf{z} \sim \tilde{q}_\phi(\cdot \mid \mathbf{x}_n)$  using the VAE's encoder to

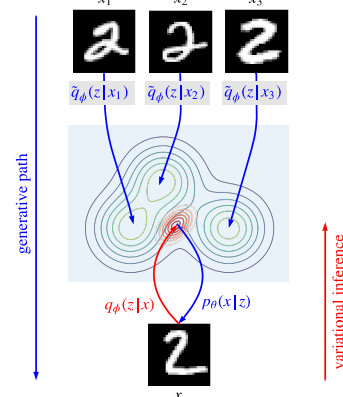


Figure 1. Exemplar VAEs generate a new sample by drawing a random exemplar  $\mathbf{x}_n$  from a training set (e.g.,  $\{\mathbf{x}_1, \mathbf{x}_2, \mathbf{x}_3\}$ ), then stochastically mapping that exemplar to the latent space by sampling from  $\tilde{q}_\phi(\mathbf{z} \mid \mathbf{x}_n)$ , followed by sampling from  $p_\theta(\mathbf{x} \mid \mathbf{z})$ . We distinguish between the variational posterior distribution  $q_\phi(\mathbf{z} \mid \mathbf{x})$  and the exemplar based latent prior distribution  $\tilde{q}_\phi(\mathbf{z} \mid \mathbf{x})$ .

transform the exemplar  $\mathbf{x}_n$  into a distribution over the latent codes, from which  $\mathbf{z}$  is drawn.

3. Sample  $\mathbf{x} \sim p_\theta(\cdot \mid \mathbf{z})$  using the VAE's decoder to transform  $\mathbf{z}$  into a distribution over the observation space, from which  $\mathbf{x}$  is drawn.

In a VAE with a Gaussian prior on latent codes, the encoder network is used during training to define a variational bound on the log marginal likelihood (Kingma & Welling, 2014). Once training is complete, a conventional VAE generates new observations using the decoder alone. To sample from an Exemplar VAE, in addition to the decoder, one needs access to a set of exemplars and the encoder, or at least the latent encoding of the exemplars. Importantly, given the non-parametric nature of Exemplar VAEs, one can train this model with one set of exemplars and perform inference with another, potentially much larger set.

Marginalizing out the exemplar index  $n$  and the latent variable  $\mathbf{z}$ , we derive an evidence lower bound (ELBO) (Jordan et al., 1999; Blei et al., 2017) on Exemplar VAE's log marginal likelihood for a single data point  $\mathbf{x}$  as:

$$\begin{aligned} & \log p(\mathbf{x}; X, \theta, \phi) \\ &= \log \sum_{n=1}^N \frac{1}{N} \int_z \tilde{q}_\phi(\mathbf{z} \mid \mathbf{x}_n) p_\theta(\mathbf{x} \mid \mathbf{z}) d\mathbf{z} \end{aligned} \quad (7)$$

$$= \log \int_z p_\theta(\mathbf{x} \mid \mathbf{z}) \sum_{n=1}^N \frac{1}{N} \tilde{q}_\phi(\mathbf{z} \mid \mathbf{x}_n) d\mathbf{z} \quad (8)$$

$$\geq \underbrace{\mathbb{E}_{q_\phi(\mathbf{z} \mid \mathbf{x})} \log p_\theta(\mathbf{x} \mid \mathbf{z})}_{\text{reconstruction}} - \underbrace{\mathbb{E}_{q_\phi(\mathbf{z} \mid \mathbf{x})} \log \frac{N q_\phi(\mathbf{z} \mid \mathbf{x})}{\sum_{n=1}^N \tilde{q}_\phi(\mathbf{z} \mid \mathbf{x}_n)}}_{\text{KL term}}. \quad (9)$$

The separation of the reconstruction and KL terms in (9) summarizes the impact of the exemplars on the learning

objective as a mixture prior distribution in the latent space, with each mixture component being defined using the latent encoding of one exemplar, i.e.,

$$r(\mathbf{z} | \{\mathbf{x}_n\}_{n=1}^N) = \sum_{j=1}^N \frac{1}{N} \tilde{q}_\phi(\mathbf{z} | \mathbf{x}_n). \quad (10)$$

This paper considers the simplest form of Exemplar VAE, with a factored Gaussian variational family and a Bernoulli observation model. Extensions to other distribution families is straightforward.

The Exemplar VAE employs two encoder networks:  $q_\phi(\mathbf{z} | \mathbf{x})$  for inference over latent codes given an observation  $\mathbf{x}$ , and  $\tilde{q}_\phi(\mathbf{z} | \mathbf{x}_n)$  for mapping an exemplar  $\mathbf{x}_n$  to the latent space to obtain an exemplar based prior. We share almost all of the parameters between  $q_\phi$  and  $\tilde{q}_\phi$ , inspired by the VAE VampPrior (Tomczak & Welling, 2018) and the derivation of ELBO with a marginal KL between the aggregated variational posterior and the prior (Hoffman & Johnson, 2016; Makhzani et al., 2015). Accordingly, we define,

$$q_\phi(\mathbf{z} | \mathbf{x}) = \mathcal{N}(\mathbf{z} | \boldsymbol{\mu}_\phi(\mathbf{x}), \boldsymbol{\Lambda}_\phi(\mathbf{x})), \quad (11)$$

$$\tilde{q}_\phi(\mathbf{z} | \mathbf{x}_n) = \mathcal{N}(\mathbf{z} | \boldsymbol{\mu}_\phi(\mathbf{x}_n), \sigma^2 \mathbf{I}), c \quad (12)$$

where the two encoders use the same Gaussian mean function  $\boldsymbol{\mu}_\phi$ , but differ in the covariance structure. The inference network uses a standard diagonal covariance matrix  $\boldsymbol{\Lambda}_\phi$ , whereas exemplar based prior uses a shared scalar parameter  $\sigma^2$  to define an isotropic Gaussian per exemplar.

To complete the definition of the learning objective for Exemplar VAEs, recall that  $\pi \sim \Pi_M^{N,i}$  represents sampling a subset of exemplars of size  $M$  uniformly at random from  $\{1, \dots, i-1, i+1, \dots, N\}$ . Incorporating subsampling regularization into (9), with some further algebraic manipulation, we obtain the following Exemplar VAE objective:

$$O_3(\theta, \phi; X) = \sum_{i=1}^N \mathbb{E}_{q_\phi(\mathbf{z} | \mathbf{x}_i)} \left[ \log \frac{p_\theta(\mathbf{x}_i | \mathbf{z})}{q_\phi(\mathbf{z} | \mathbf{x}_i)} + \mathbb{E}_{\Pi_M^{N,i}(\pi)} \log r(\mathbf{z} | \{\mathbf{x}_{\pi_m}\}_{m=1}^M) \right], \quad (13)$$

with the aggregated exemplar based prior  $r(\cdot | X)$  defined as

$$\log r(\mathbf{z} | \{\mathbf{x}_j\}_{j=1}^M) = \log \sum_{j=1}^M \exp \frac{-\|\mathbf{z} - \boldsymbol{\mu}_\phi(\mathbf{x}_j)\|^2}{2\sigma^2} - \log C - \log M, \quad (14)$$

where  $\log C = d_z \log(\sqrt{2\pi}\sigma)$ . For learning, we use a single Monte Carlo sample per data point and the reparameterization trick to estimate the gradient of (13) with respect to  $\mathbb{E}_{q_\phi(\mathbf{z} | \mathbf{x}_i)}$ . In other words,  $\mathbf{z}$  in (13) is obtained via a stochastic latent encoding of a data point  $\mathbf{x}$  using  $\epsilon \sim \mathcal{N}(0, \mathbf{I})$  and  $\mathbf{z} = \boldsymbol{\mu}_\phi(\mathbf{x}) + \boldsymbol{\Lambda}_\phi(\mathbf{x})^{1/2} \epsilon$  for a diagonal  $\boldsymbol{\Lambda}$ .

The simplicity of the Gaussian mixture prior in (14) enables efficient computation of all of the pairwise distances between a minibatch of latent codes  $\{\mathbf{z}_b\}_{b=1}^B$  and Gaussian means  $\{\boldsymbol{\mu}_\phi(\mathbf{x}_j)\}_{j=1}^M$  using a single matrix product. Moreover, it makes it possible to rely on existing approximate nearest neighbor search methods in the Euclidean to speed up training space (e.g., Muja & Lowe (2014)).

Recall the definition of Parzen window estimates using Gaussian kernels in (2) and note the similarity between (2) and (14). The Exemplar VAE’s Gaussian mixture prior can be thought of as a Parzen window estimate in the latent space. Therefore, Exemplar VAEs can be interpreted as *deep Parzen window estimators*, which learn a latent space well suited to Parzen window density estimation.

### 3.1. Approximate Nearest Neighbor Search for Efficient Optimization

The computational cost during training can become a burden as the number of exemplars ( $M$ ) increases. As explained next, this can be mitigated with the use of fast, approximate nearest neighbor search in the latent space to find subsets of relevant items, providing a lower bound on the ELBO.

For each training point  $\mathbf{x}_i$ , we sample  $\pi \sim \Pi_M^{N,i}$  and then compute (14). As an alternative, rather than using all  $M$  exemplars, one could evaluate each  $\mathbf{x}_i$  with respect to  $k$  nearest neighbors in the latent space, where  $k \ll M$ . Back propagation is therefore faster, and because probability density is non-negative and log is monotonically increasing, it follows that

$$\begin{aligned} \log r(\mathbf{z} | \{\mathbf{x}_{\pi_m}\}_{m=1}^M) &= \log \sum_{m=1}^M \frac{1}{N} \tilde{q}_\phi(\mathbf{z} | \mathbf{x}_m) \\ &\geq \log \sum_{j \in (k\text{NN} \cap M)} \frac{1}{N} \tilde{q}_\phi(\mathbf{z} | \mathbf{x}_j). \end{aligned} \quad (15)$$

That is, approximating the exemplar prior with  $k$  nearest neighbors is a lower bound on the log prior term and (13).

We store a cache of latent codes for training points to facilitate nearest neighbor search. The cache is updated whenever a new latent code of a training point is available, i.e., we update the cache for any points in the training minibatch and the prior batch kNN as they are passed through the encoder. Algorithm 1 summarizes the efficient learning procedure.

## 4. Related Work

Variational Autoencoders (VAEs) (Kingma & Welling, 2014; Rezende et al., 2014) are a versatile class of latent variable generative models used for non-linear dimensionality reduction (Gregor et al., 2016), generating discrete data (Bowman et al., 2015), and learning disentangled representations (Higgins et al., 2016; Chen et al., 2018), while providing a

**Algorithm 1** Efficient Exemplar VAE Learning Algoirthm

---

**Input:** Training dataset  $\mathcal{X} = \{\mathbf{x}_n\}_{n=1}^N$

**Define** Cache:

- initialize cache = []
- insert( $i, c$ ): insert value  $c$  with index  $i$  into cache
- update( $i, c$ ): update the value of index  $i$  to  $c$
- kNN( $c$ ): return indices of kNNs of  $c$  in cache

**for**  $n$  **in**  $\{1, \dots, N\}$  **do** Cache.insert( $n, \mu_\phi(\mathbf{x}_n)$ )

**for** epoch **in**  $\{1, \dots, L\}$  **do**

- for**  $i$  **in**  $\{1, \dots, N\}$  **do**
- $\pi \sim \Pi_M^{N,i}$  to obtain a set of  $M$  exemplar indices
- $\mu_i, \Lambda_i = \mu_\phi(\mathbf{x}_i), \Lambda_\phi(\mathbf{x}_i)$
- $\epsilon \sim \mathcal{N}(0, I_{d_z \times d_z})$
- $\mathbf{z} = \mu_i + \Lambda_i^{1/2} \epsilon$
- kNN = Cache.kNN( $\mu_i$ )  $\cap \pi$
- for**  $j$  **in** kNN **do**  $\mu_j = \mu_\phi(\mathbf{x}_j)$
- $r(\mathbf{z}) = \frac{1}{M} \sum_{j \in \text{kNN}} \mathcal{N}(\mathbf{z} | \mu_j, \sigma^2)$
- ELBO =  $\log p_\theta(\mathbf{x} | \mathbf{z}) - \log \mathcal{N}(\mathbf{z} | \mu_i, \Lambda_i) + \log r(\mathbf{z})$
- Gradient ascend on ELBO to update  $\phi$ ,  $\theta$ , and  $\sigma^2$
- Cache.update( $i, \mu_i$ )
- for**  $j$  **in** kNN **do** Cache.update( $j, \mu_j$ )

---

tractable lower bound on the log marginal likelihood. Improved variants of the VAE have been proposed through modifications to the VAE objective function (Burda et al., 2015), more flexible variational familieis (Kingma et al., 2016; Rezende & Mohamed, 2015), and more powerful decoding models (Chen et al., 2016; Gulrajani et al., 2016).

In particular, recent work shows that more powerful latent priors (Tomczak & Welling, 2018; Bauer & Mnih, 2018; Dai & Wipf, 2019; Lawson et al., 2019) can significantly improve the effectiveness of VAEs for density estimation, as was hinted by (Hoffman & Johnson, 2016). This line of work is motivated in part by the empirical observation of the gap between the prior and the aggregated posterior (e.g., Makhzani et al. (2015)). Using more powerful latent priors may help avoid posterior collapse, which is a barrier to the use of VAEs with autoregressive decoders (Bowman et al., 2015). Unlike most existing work, the Exemplar VAE makes limited assumptions about the structure of the latent space and uses a non-parametric exemplar based prior in the latent space.

VAEs with a VampPrior (Tomczak & Welling, 2018) optimize a set of pseudo-inputs together with the encoder network to obtain a mixture model approximation to the aggregate posterior. They argue that computing the exact aggregated posterior is expensive and suffers from overfitting; to avoid overfitting they ensure that  $K \ll N$ . VampPrior and Exemplar VAE are similar in their reuse of the encoding network and a mixture distribution over the latent space. Exemplar VAE does not require an increase in the number of

model parameters, and it avoids overfitting through simple but effective regularization techniques (Sec. 2). Computational costs are reduced through approximate kNN search during training. Exemplar VAE also extends naturally to large high dimensional datasets, and to discrete data, which are challenging for pseduo-input optimization.

Attention and external memory are effective elements in deep learning architectures. Li et al. (2016) used memory augmented networks with attention to enhance generative models. Bornschein et al. (2017) used hard attention with memory in a VAE, with generation conditioned on a sample from the memory, using both learnable and exemplar memory. One can view Exemplar VAE as a VAE augmented with memory. Exemplar VAE and (Bornscchein et al., 2017) are similar in conditioning generation on external samples. Bornschein et al. (2017) optimized for a discrete variable to select the suitable memory index, which can be challenging. In contrast, we use a uniform distribution over exemplars, and computation costs are reduced through approximate KNN search in latent space. Further, their formulation of the variational posterior is a barrier to sharing the encoder between the approximate posterior and the memory addressing component, unlike VampPrior and Exemplar VAE.

While introduced in the context of VAEs, the use of exemplar based generative models is not limited to VAEs. Indeed, one can extend the use of exemplar based priors to other powerful generative frameworks, such as Normalizing Flow (Dinh et al., 2016; 2014; Kingma & Dhariwal, 2018). For example, Li et al. (2019) propose to exploit the local manifold of data points in the latent space to improve Normalizing Flow. They use a simple distance metric based on PCA to define the neighborhood structure. Here, we show that one can train models in an end-to-end manner and let the network design the distance metric.

In natural language processing Guu et al. (2018) propose a way to edit samples from training corpus in terms of a neural editor, given a sentence and an edit vector. For each training sentence, they consider a set of similar prototypes selected based on Jaccard distance. This is similar in spirit to the Exemplar VAE, however, like Li et al. (2019), they pre-specify rather than learn the distance metric. Following (Guu et al., 2018; Li et al., 2019), we cast the global generation problem into one of transforming data points. This also bridges the gap between data augmentation and generation.

## 5. Experiments

To assess the effectiveness of Exemplar VAEs we conduct three sets of experiments, on density estimation, representation learning, and unsupervised data augmentation.

**Experimental setup.** For training generative models, we mirror the experimental setup of the VampPrior (Tom-

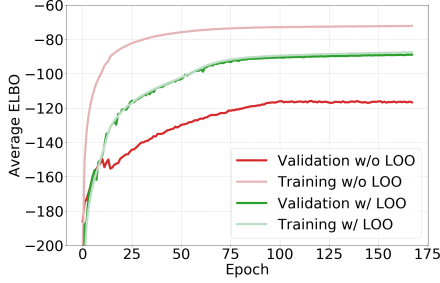


Figure 2. Training and validation ELBO on Dynamic MNIST for Exemplar VAE with and without LOO. LOO reduces the generalization gap between training and validation ELBO.

czak & Welling, 2018) as much as possible. We use the same hyper-parameters and optimizers (gradient normalized Adam (Kingma & Ba, 2014; Yu et al., 2017a)), but we change the generative model. We use a learning rate of 5e-4. We stop training if for 50 consecutive epochs the validation ELBO does not improve. Dynamic binarization of training data is used. We use linear KL annealing for 100 epochs.

MNIST comprising 50K training and 10K validation images. For Omniglot, 1345 randomly selected points are used for validation; the 23K remaining images are used for training. All results reported for VampPrior and VAE with Gaussian prior are based on the github implementation of VampPrior generously provided by the authors. Below we consider three architectures: In VAE we use an MLP with 2 hidden layers (300 units each) both for encoder and decoder. HVAE has two stochastic layers, where the generative distribution is  $p_\phi(\mathbf{z}_2)p_\phi(\mathbf{z}_1 | \mathbf{z}_2)p_\phi(\mathbf{x} | \mathbf{z}_1, \mathbf{z}_2)$ , and the approximate posterior is  $q_\phi(\mathbf{z}_1 | \mathbf{x}, \mathbf{z}_2)q_\phi(\mathbf{z}_2 | \mathbf{x})$ . Like the VAE, the encoders and decoders are MLPs. We fix the prior over  $\mathbf{z}_1$  to a standard Gaussian and use more expressive priors just for  $p(z_2)$ . ConvHVAE is more powerful. Its generative and posterior distributions are like HVAE, but with convolutional layers. Details about the architectures and hyper-parameters are given in the supplementary material.

**Evaluation.** For evaluation of density models, we use the multi-sample bound in Importance Weighted Autoencoders (IWAE) (Burda et al., 2015) with 5000 samples to lower bound the log probability of test data. We use the whole training dataset as the exemplar set, without any regularization or kNN acceleration. This makes the evaluation time consuming, but generating an unbiased sample from the Exemplar VAE is efficient. Our preliminary experiments suggest that using kNN for evaluation is feasible.

### 5.1. Ablation Study

First, we evaluate the effectiveness of the regularization techniques proposed (Sec. 2), e.g., leave-one-out and exemplar subsampling, for enhancing generalization.

**Leave-one-out.** Here we consider a VAE trained with an optimal prior (aggregated posterior) and report the gap be-

tween the ELBO computed on the training and validation sets. The VampPrior has shown that increasing the number of pseudo-inputs causes overfitting, but here we consider an exact optimal prior. Fig. 2 demonstrates the effectiveness of leave-one-out in helping to avoid overfitting. Table 1 gives the test log-likelihood lower bounds for Exemplar VAE on both MNIST and Omniglot with and without LOO.

Dataset	Exemplar VAE	
	w/ LOO	w/o LOO
MNIST	-82.35	-101.33
Omniglot	-105.80	-139.12

Table 1. Log likelihood lower bounds on the test set (in nats) for Exemplar VAE with and without leave-one-out (LOO).

**Exemplar subsampling.** As explained in Section 2, the Exemplar VAE uses a hyper-parameter  $M$  to define the number of exemplars used for estimating the prior. Here, we report the Exemplar VAE’s performance as a function of  $M$  divided by the number of training data points  $N$ . We consider  $M/N \in \{1, 0.5, 0.2, 0.1\}$ . All models employ LOO, so the use of  $M/N = 1$  refers to  $M = N - 1$ . Table 2 presents the results for both MNIST and Omniglot. In all of the following experiments we will use  $M/N = 0.5$ .

Dataset	$M/N$			
	1	0.5	0.2	0.1
MNIST	-82.35	<b>-82.09</b>	-82.12	-82.20
Omniglot	-105.80	-105.22	<b>-104.95</b>	-105.42

Table 2. Log likelihood lower bounds on the test set (in nats) for Exemplar VAE with different fractions of exemplar subsampling.

**Efficient learning.** For simple VAE architectures, finding the exact prior probability of latent codes based on (10), even for  $M \approx 50K$ , is feasible. We use this opportunity to ablate the use of approximate nearest neighbor search and caching for efficient training. Table 4 shows that Efficient Exemplar VAE is competitive with vanilla Exemplar VAE.

### 5.2. Density Estimation

We report density estimation with MNIST, Omniglot and Fashion MNIST, using three different architectures, namely VAE, HVAE and ConvHVAE (Tomczak & Welling, 2018). For each architecture we consider a Gaussian prior, the VampPrior, and an Exemplar based prior. For training VAE and HVAE we used the exact exemplar prior, but for ConvHVAE we used 10NN exemplars (see Sec. 3.1).

Table 3 shows that Exemplar VAE outperforms other models (in all but one case), including the VampPrior which represents the state-of-the-art among VAEs with a factored variational posterior. Improvements of Exemplar VAE on Omniglot data are greater than on other datasets, which is

Exemplar VAEs for Exemplar based Generation and Data Augmentation

Method	Dynamic MNIST	Fashion MNIST	Omniglot
VAE w/ Gaussian prior	$-84.45 \pm 0.12$	$-228.70 \pm 0.15$	$-108.34 \pm 0.06$
VAE w/ VampPrior	$-82.43 \pm 0.06$	$-227.35 \pm 0.05$	$-106.78 \pm 0.21$
Exemplar VAE	<b><math>-82.09 \pm 0.18</math></b>	<b><math>-226.75 \pm 0.07</math></b>	<b><math>-105.22 \pm 0.18</math></b>
HVAE w/ Gaussian prior	$-82.39 \pm 0.11$	$227.37 \pm 0.1$	$-104.92 \pm 0.08$
HVAE w/ VampPrior	$-81.56 \pm 0.09$	$-226.72 \pm 0.08$	$-103.30 \pm 0.43$
Exemplar HVAE	<b><math>-81.22 \pm 0.05</math></b>	<b><math>-226.53 \pm 0.09</math></b>	<b><math>-102.25 \pm 0.43</math></b>
ConvHVAE w/ Gaussian prior	$-80.52 \pm 0.28$	$-225.38 \pm 0.08$	$-98.12 \pm 0.17$
ConvHVAE w/ Lars	$-80.30$	$-225.92$	$-97.08$
ConvHVAE w/ SNIS	$-79.91 \pm 0.05$	$-225.35 \pm 0.07$	N/A
ConvHVAE w/ VampPrior	$-79.67 \pm 0.09$	$-224.67 \pm 0.03$	$-97.30 \pm 0.07$
Exemplar ConvHVAE	<b><math>-79.58 \pm 0.07</math></b>	<b><math>-224.63 \pm 0.06</math></b>	<b><math>-96.38 \pm 0.24</math></b>

Table 3. Density estimation on dynamic MNIST, Fashion MNIST, and Omniglot for different methods and architectures. Log likelihood lower bounds (in nats) averaged across 5 training runs are estimated using IWAE with 5000 samples. All of the architectures use 40-dimensional latent spaces. For LARS (Bauer & Mnih, 2018) and SNIS (Lawson et al., 2019), the IWAE is computed based on 1000 (vs 5000) samples; their architectures and training procedures are also somewhat different.

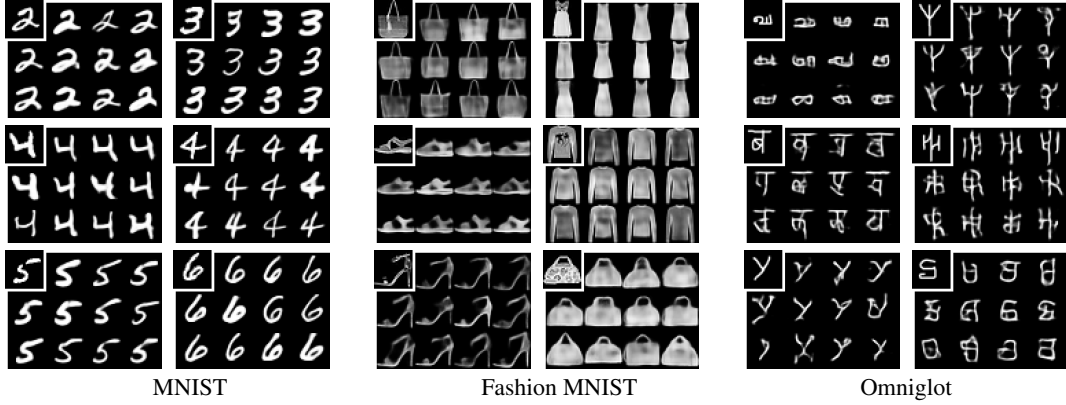


Figure 3. Given the input exemplar on the top left of each plate, 11 conditional Exemplar VAE samples are generated and shown. The Exemplar VAE is able to generate diverse samples while typically preserving the class label and the style of the input exemplar.

Model	M/N			
	1	0.5	0.2	0.1
Exemplar VAE	-82.35	-82.09	-82.12	-82.2
kNN Exemplar VAE	-82.32	-82.15	-82.07	-82.07

Table 4. Log likelihood lower bounds on the test set (in nats) for Exemplar VAE and kNN Exemplar VAE with k=10.

likely due to the significant diversity of this dataset. One can enhance VampPrior with more pseudo-inputs, but we find this often makes optimization challenging and leads to overfitting. We posit that, by comparison, Exemplar VAEs have the potential to scale more easily to large, diverse datasets.

Fig. 10 shows samples generated from Exemplar ConvVAE (top-left is the input exemplar for each plate). These samples highlight the power of Exemplar VAE in maintaining the content of the source image while adding diversity. In the case of MNIST the most evident changes are in the stroke width and brightness with slight variation in shape. Fashion MNIST and Omniglot samples show more pronounced

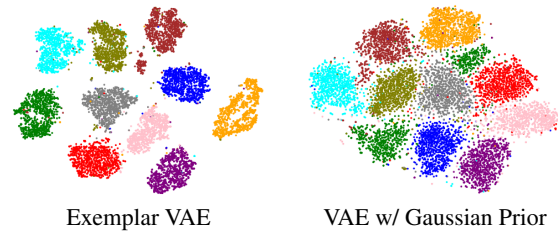


Figure 4. t-SNE visualization of learned latent representations for MNIST test points, colored by labels.

variations to the style of the source image, possibly because both datasets exhibit greater diversity than MNIST.

### 5.3. Representation Learning

We next explore the structure of the latent representation for Exemplar VAE. Fig. 4 shows a t-SNE visualization of the latent representations of MNIST test data for the Exemplar VAE and for VAE with a Gaussian prior. Test points are colored by their digit label. (No labels were used during training.) The Exemplar VAE representation appears more meaningful, with tighter clusters. We also use k-nearest

## Exemplar VAEs for Exemplar based Generation and Data Augmentation

Method	MNIST	Fashion MNIST
VAE w/ Gaussian Prior	$2.41 \pm 0.27$	$15.90 \pm 0.34$
VAE w/ VampPrior	$1.42 \pm 0.02$	$12.74 \pm 0.18$
Exemplar VAE	<b><math>1.13 \pm 0.06</math></b>	<b><math>12.56 \pm 0.08</math></b>

Table 5. kNN classification error (%) on 40-D representations.

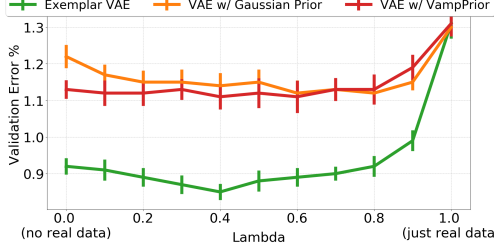


Figure 5. MNIST validation error as a function of  $\lambda$  in (16) for different generative models. The parameter  $\lambda$  controls the strength of the loss on real vs. augmented data. Here, we use a simple MLP with ReLU activations and two hidden layers of 1024 units.

neighbor (kNN) classification performance as a proxy for the representation quality. As is clear from Table 5, Exemplar VAE consistently outperforms other approaches. Results on Omniglot are not reported since the low resolution version of this dataset does not include class labels.

### 5.4. Generative Data Augmentation

We assess the effectiveness of the Exemplar VAE for generating augmented data to improve supervised learning. Recent generative models have achieved impressive sample quality and diversity, but they have seen limited success in improving discriminative models. Ravuri & Vinyals (2019) used class-conditional generative models to synthesize extra training data, yielding marginal gains on ImageNet accuracy. Alternative techniques for optimizing data augmentation policies (Cubuk et al., 2019; Lim et al., 2019; Hataya et al., 2019) or approaches based on adversarial perturbations (Goodfellow et al., 2014b; Miyato et al., 2018) have been more successful in improving classification accuracy.

In our experiments we use the training data points as exemplars and generate additional samples from the Exemplar VAE. Class labels of the exemplars are transferred to corresponding new images, and a combination of real and generated data is used for training. More specifically, during each training iteration, we follow the following steps:

1. Draw a minibatch  $X = \{(\mathbf{x}_i, y_i)\}_{i=1}^B$  from training data.
2. For each  $\mathbf{x}_i \in X$ , draw  $\mathbf{z}_i \sim \tilde{q}(\mathbf{z} \mid \mathbf{x}_i)$ , and then set  $\tilde{\mathbf{x}}_i = p_\phi(\mathbf{x} \mid \mathbf{z}_i)$ , which inherits the class label  $y_i$ . This yields a synthetic minibatch  $\tilde{X} = \{(\tilde{\mathbf{x}}_i, y_i)\}_{i=1}^B$ .
3. Gradient descend on the weighted cross entropy loss,

$$\ell = - \sum_{i=1}^B \left[ \lambda \log p_\theta(y_i \mid \mathbf{x}_i) + (1-\lambda) \log p_\theta(y_i \mid \tilde{\mathbf{x}}_i) \right] \quad (16)$$

Method	Hidden layers	Test error
Dropout [1]	$3 \times 1024$	1.25
Label smoothing [2]	$2 \times 1024$	$1.23 \pm 0.06$
Dropconnect [3]	$2 \times 800$	1.20
Variational Info. Bottleneck [4]	$2 \times 1024$	1.13
Dropout + Max norm constraint [1]	$2 \times 8192$	0.95
Manifold Tangent Classifier [5]	$2 \times 2000$	0.81
DBM + dropout finetuning [1]	500-500-2000	0.79
Label Smoothing (LS)	$2 \times 1024$	$1.23 \pm 0.01$
LS + Exemplar VAE Augmentation	$2 \times 1024$	$0.77 \pm 0.01$
Label Smoothing	$2 \times 8196$	$1.17 \pm 0.01$
LS + Exemplar VAE Augmentation	$2 \times 8192$	<b><math>0.69 \pm 0.01</math></b>

Table 6. Test error (%) on permutation invariant MNIST from [1] Srivastava et al. (2014), [2] Pereyra et al. (2017), [3] Wan et al. (2013), [4] Alemi et al. (2016), and [5] Rifai et al. (2011), as well as our results with and without generative data augmentation.

Method	Hidden layers	Test error
Label Smoothing	$2 \times 1024$	$9.03 \pm 0.05$
LS + Exemplar VAE Augmentation	$2 \times 1024$	$8.52 \pm 0.03$
Label Smoothing	$2 \times 8196$	$8.56 \pm 0.03$
LS + Exemplar VAE Augmentation	$2 \times 8192$	<b><math>8.16 \pm 0.03</math></b>

Table 7. Test error (%) on permutation invariant Fashion MNIST.

We train MLPs with ReLU activations and two hidden layers of 1024 or 8192 units on MNIST and Fashion MNIST, using the proposed generative data augmentation method. We leverage label smoothing (Szegedy et al., 2016) with a smoothing parameter of 0.1 for our experiments with and without data augmentation. Note that the Exemplar VAEs used for data augmentation adopt fully connected layers and do not observe class labels during training. Networks are optimized using stochastic gradient descent with a momentum of 0.9 for 100 epochs. The learning rate is linearly decayed from an initial value of  $\eta$  to  $\eta/100$ . The meta-parameters  $\lambda$  in (16) and  $\eta$  were tuned using the validation set.

Figure 5 shows that Exemplar VAE is far more effective than other VAEs for data augmentation and even a small amounts of generative data augmentation improves classifier accuracy. Interestingly, a classifier trained solely on synthetic data achieves error rates smaller than classifiers trained on the original data. Given  $\eta = 0.1$ ,  $\lambda = 0.4$  on MNIST and  $\lambda = 0.8$  on Fashion MNIST, we train 10 networks on the union of training and validation sets and report average test errors. On permutation invariant MNIST, Exemplar VAE augmentations achieve an impressive average error rate of 0.69%. Table 6 summarizes our results in comparison with previous work. On MNIST, Ladder Networks (Sønderby et al., 2016) and Virtual Adversarial Training (Miyato et al., 2018) report 0.57% and 0.64% error rates respectively, using deeper architectures and much more complex training procedures. Table 7 summarizes our results on permutation invariant Fashion MNIST, showing consistent gains stemming from Exemplar VAE augmentations.

## 6. Conclusion

This paper develops a new framework for exemplar based generative modeling. We extend this framework to VAEs, based on which we define an Exemplar based prior distribution on latent variables. We present two simple but efficacious regularization techniques for Exemplar VAEs. An efficient learning algorithm based on approximate nearest neighbor search is proposed. The effectiveness of the Exemplar VAE on density estimation, representation learning, and data augmentation for supervised learning is demonstrated.

The development of Exemplar VAEs opens up interesting future research directions. Application to language modeling and other discrete data, especially in the context of unsupervised data augmentation is worth exploring. Extensions to other generative models such as Normalizing FLoW and GANs, and larger and more complex image datasets are promising. Exploring the effect of the exemplar based prior on posterior collapse and learning disentangled representations would be valuable. Last but not least, the non-parametric properties of Exemplar VAE may enable evaluation of generative models with intractable log-likelihoods.

## Acknowledgement

We are extremely grateful to Micha Livne, Will Grathwohl, and Kevin Swersky for extensive discussions. We thank Diederik Kingma, Chen Li, and Danijar Hafner for their feedback on an initial draft of this paper. This work was financially supported in part by a grant from NSERC Canada.

## References

Alemi, A. A., Fischer, I., Dillon, J. V., and Murphy, K. Deep variational information bottleneck. *arXiv:1612.00410*, 2016.

Bauer, M. and Mnih, A. Resampled priors for variational autoencoders. *arXiv:1810.11428*, 2018.

Blei, D. M., Kucukelbir, A., and McAuliffe, J. D. Variational inference: A review for statisticians. *Journal of the American Statistical Association*, 2017.

Bornschein, J., Mnih, A., Zoran, D., and Rezende, D. J. Variational memory addressing in generative models. *NeurIPS*, 2017.

Bowman, S. R., Vilnis, L., Vinyals, O., Dai, A. M., Jozefowicz, R., and Bengio, S. Generating sentences from a continuous space. *arXiv:1511.06349*, 2015.

Burda, Y., Grosse, R., and Salakhutdinov, R. Importance weighted autoencoders. *arXiv:1509.00519*, 2015.

Chen, R. T. Q., Li, X., Grosse, R., and Duvenaud, D. Isolating sources of disentanglement in variational autoencoders. *Advances in Neural Information Processing Systems*, 2018.

Chen, X., Kingma, D. P., Salimans, T., Duan, Y., Dhariwal, P., Schulman, J., Sutskever, I., and Abbeel, P. Variational lossy autoencoder. *arXiv:1611.02731*, 2016.

Criminisi, A., Perez, P., and Toyama, K. Object removal by exemplar-based inpainting. *CVPR*, 2003.

Cubuk, E. D., Zoph, B., Mane, D., Vasudevan, V., and Le, Q. V. Autoaugment: Learning augmentation strategies from data. *Computer Vision and Pattern Recognition*, pp. 113–123, 2019.

Dai, B. and Wipf, D. Diagnosing and enhancing VAE models. *ICLR*, 2019.

Dauphin, Y. N., Fan, A., Auli, M., and Grangier, D. Language modeling with gated convolutional networks. *International Conference on Machine Learning*, 70:933–941, 2017.

Dinh, L., Krueger, D., and Bengio, Y. Nice: Non-linear independent components estimation. *arXiv:1410.8516*, 2014.

Dinh, L., Sohl-Dickstein, J., and Bengio, S. Density estimation using real nvp. *arXiv:1605.08803*, 2016.

Efros, A. A. and Leung, T. K. Texture synthesis by non-parametric sampling. *International Conference on Computer Vision*, 1999.

Freeman, W. T., Jones, T. R., and Pasztor, E. C. Example-based super-resolution. *IEEE Computer graphics and Applications*, 2002.

Goodfellow, I., Pouget-Abadie, J., Mirza, M., Xu, B., Warde-Farley, D., Ozair, S., Courville, A., and Bengio, Y. Generative adversarial nets. *Advances in neural information processing systems*, pp. 2672–2680, 2014a.

Goodfellow, I. J., Shlens, J., and Szegedy, C. Explaining and harnessing adversarial examples. *arXiv:1412.6572*, 2014b.

Gregor, K., Besse, F., Rezende, D. J., Danihelka, I., and Wierstra, D. Towards conceptual compression. *NeurIPS*, 2016.

Gulrajani, I., Kumar, K., Ahmed, F., Taiga, A. A., Visin, F., Vazquez, D., and Courville, A. Pixelvae: A latent variable model for natural images. *arXiv:1611.05013*, 2016.

Guu, K., Hashimoto, T. B., Oren, Y., and Liang, P. Generating sentences by editing prototypes. *TACL*, 2018.

Hataya, R., Zdenek, J., Yoshizoe, K., and Nakayama, H. Faster autoaugment: Learning augmentation strategies using backpropagation. *arXiv:1911.06987*, 2019.

Hays, J. and Efros, A. A. Scene completion using millions of photographs. *ACM Transac. on Graphics (TOG)*, 2007.

Higgins, I., Matthey, L., Pal, A., Burgess, C., Glorot, X., Botvinick, M., Mohamed, S., and Lerchner, A. beta-VAE: Learning basic visual concepts with a constrained variational framework. *International Conference on Learning Representations*, 2016.

Hoffman, M. D. and Johnson, M. J. Elbo surgery: Yet another way to carve up the variational evidence lower bound. *Workshop in Advances in Approximate Bayesian Inference, NIPS*, 1:2, 2016.

Johnson, J., Alahi, A., and Fei-Fei, L. Perceptual losses for real-time style transfer and super-resolution. *ECCV*, 2016.

Jordan, M. I., Ghahramani, Z., Jaakkola, T. S., and Saul, L. K. An introduction to variational methods for graphical models. *Machine Learning*, 1999.

Khandelwal, U., Levy, O., Jurafsky, D., Zettlemoyer, L., and Lewis, M. Generalization through memorization: Nearest neighbor language models. *arXiv:1911.00172*, 2019.

Kingma, D. P. and Ba, J. Adam: A method for stochastic optimization. *arXiv:1412.6980*, 2014.

Kingma, D. P. and Dhariwal, P. Glow: Generative flow with invertible 1x1 convolutions. *Advances in Neural Information Processing Systems*, pp. 10215–10224, 2018.

Kingma, D. P. and Welling, M. Auto-encoding variational bayes. *ICLR*, 2014.

Kingma, D. P., Salimans, T., Jozefowicz, R., Chen, X., Sutskever, I., and Welling, M. Improved variational inference with inverse autoregressive flow. *NeurIPS*, 2016.

Kunin, D., Bloom, J. M., Goeva, A., and Seed, C. Loss landscapes of regularized linear autoencoders. *arXiv:1901.08168*, 2019.

Lafferty, J., McCallum, A., and Pereira, F. C. Conditional random fields: Probabilistic models for segmenting and labeling sequence data. *ICML*, 2001.

Lawson, J., Tucker, G., Dai, B., and Ranganath, R. Energy-inspired models: Learning with sampler-induced distributions. *NeurIPS*, 2019.

Li, C., Zhu, J., and Zhang, B. Learning to generate with memory. *ICML*, 2016.

Li, Y., Gao, T., and Oliva, J. A forest from the trees: Generation through neighborhoods. *arXiv:1902.01435*, 2019.

Lim, S., Kim, I., Kim, T., Kim, C., and Kim, S. Fast autoaugment. *NeurIPS*, 2019.

Lucas, J., Tucker, G., Grosse, R. B., and Norouzi, M. Don't blame the elbo! a linear vae perspective on posterior collapse. *NeurIPS*, 2019.

Makhzani, A., Shlens, J., Jaitly, N., Goodfellow, I., and Frey, B. Adversarial autoencoders. *arXiv:1511.05644*, 2015.

Miyato, T., Maeda, S.-i., Koyama, M., and Ishii, S. Virtual adversarial training: A regularization method for supervised and semi-supervised learning. *IEEE Trans. PAMI*, 41(8):1979–1993, 2018.

Muja, M. and Lowe, D. G. Scalable nearest neighbor algorithms for high dimensional data. *IEEE Trans. PAMI*, 2014.

Oord, A. v. d., Dieleman, S., Zen, H., Simonyan, K., Vinyals, O., Graves, A., Kalchbrenner, N., Senior, A., and Kavukcuoglu, K. Wavenet: A generative model for raw audio. *arXiv:1609.03499*, 2016.

Parzen, E. On estimation of a probability density function and mode. *Annals of Mathematical Statistics*, 1962.

Pereyra, G., Tucker, G., Chorowski, J., Kaiser, Ł., and Hinton, G. Regularizing neural networks by penalizing confident output distributions. *arXiv:1701.06548*, 2017.

Ravuri, S. and Vinyals, O. Classification accuracy score for conditional generative models. *Advances in Neural Information Processing Systems*, pp. 12247–12258, 2019.

Reed, S., Akata, Z., Yan, X., Logeswaran, L., Schiele, B., and Lee, H. Generative adversarial text to image synthesis. *ICLR*, 2016.

Rezende, D. J. and Mohamed, S. Variational inference with normalizing flows. *arXiv:1505.05770*, 2015.

Rezende, D. J., Mohamed, S., and Wierstra, D. Stochastic backpropagation and approximate inference in deep generative models. *arXiv:1401.4082*, 2014.

Rifai, S., Dauphin, Y. N., Vincent, P., Bengio, Y., and Muller, X. The manifold tangent classifier. *Advances in Neural Information Processing Systems*, pp. 2294–2302, 2011.

Sønderby, C. K., Raiko, T., Maaløe, L., Sønderby, S. K., and Winther, O. Ladder variational autoencoders. *Advances in Neural Information Processing Systems*, pp. 3738–3746, 2016.

Srivastava, N., Hinton, G., Krizhevsky, A., Sutskever, I., and Salakhutdinov, R. Dropout: a simple way to prevent neural networks from overfitting. *JMLR*, 2014.

Szegedy, C., Vanhoucke, V., Ioffe, S., Shlens, J., and Wojna, Z. Rethinking the inception architecture for computer vision. *Proceedings of the IEEE conference on computer vision and pattern recognition*, 2016.

Tomczak, J. M. and Welling, M. Vae with a vampprior. *AISTATS*, 2018.

Wan, L., Zeiler, M., Zhang, S., Le Cun, Y., and Fergus, R. Regularization of neural networks using dropconnect. *International Conference on Machine Learning*, pp. 1058–1066, 2013.

Xing, E. P., Jordan, M. I., Russell, S. J., and Ng, A. Y. Distance metric learning with application to clustering with side-information. *NeurIPS*, 2003.

Yu, A. W., Huang, L., Lin, Q., Salakhutdinov, R., and Carbonell, J. Block-normalized gradient method: An empirical study for training deep neural network. *arXiv:1707.04822*, 2017a.

Yu, A. W., Lin, Q., Salakhutdinov, R., and Carbonell, J. Normalized gradient with adaptive stepsize method for deep neural network training. *arXiv:1707.04822*, 18(1), 2017b.

## A. Number of Active Dimensions in the Latent Space

The problem of posterior collapse (Bowman et al., 2015; Lucas et al., 2019), resulting in a number of inactive dimensions in the latent space of a VAE, can be reduced via the use a VampPrior (Tomczak & Welling, 2018) as opposed to a factored Gaussian prior. We also investigate this phenomena by counting the number of active dimensions based on a metric proposed by Burda et. al (Burda et al., 2015). This metric computes the variance of the mean of the latent encoding of the data points in each dimension of the latent space,  $\text{Var}(\mu_\phi(\mathbf{x})_i)$ , where  $\mathbf{x}$  is sampled from the dataset. If the computed variance is above a certain threshold, then that dimension is considered active. The proposed threshold by (Bauer & Mnih, 2018) is 0.01 and we use the same value. We observe that the Exemplar VAE has the largest number of active dimensions in all cases except one. In the case of ConvHVAE on MNIST and Fashion MNIST, the gap between Exemplar VAE and other methods is more considerable.

Model	Number of Active Dimensions out of 40		
	Dynamic MNIST	Fashion MNIST	Omniglot
VAE w/ Gaussian prior	24.0±0.63	26.0±1.1	35.2±0.4
VAE w/ VampPrior	27.6±1.36	35.25±1.3	<b>40.0±0.0</b>
Exemplar VAE	<b>29.4±0.49</b>	<b>36.0±1.41</b>	<b>40.0±0.0</b>
HVAE w/ Gaussian prior	15.0±0.63	12.4±0.8	24.8±1.83
HVAE w/ VampPrior	20.4±0.49	23.2±1.47	<b>39.0±0.89</b>
Exemplar HVAE	<b>21.6±0.49</b>	<b>28.6±0.8</b>	38.6±1.5
ConvHVAE w/ Gaussian prior	19.8±2.93	15.4±2.65	39.2±1.6
ConvHVAE w/ VampPrior	19.0±1.55	19.25±0.83	39.8±0.4
Exemplar ConvHVAE	<b>25.8±3.66</b>	<b>33.6±7.86</b>	<b>40.0±0.0</b>

Table 8. The number of active dimensions computed based on a metric proposed by Burda et. al (Burda et al., 2015). This metric considers a latent dimension active if the variance of its mean over the dataset is higher than 0.01. For hierarchical architectures the reported number is for the  $\mathbf{z}_2$  which is the highest stochastic layer.

## B. Cyclic Generation

The exemplar VAE generates a new sample by transforming a randomly selected exemplar. The newly generated data point can also be used as an exemplar and we can repeat this procedure again and again. This kind of generation bears some similarity to MCMC in energy-based models. Figure 6 shows how samples evolve and consistently stay near the manifold of MNIST digits. We can apply the same procedure starting from a noisy input image as an exemplar. Figure 7 shows that the model is able to quickly transform the noisy images into samples that resemble real MNIST images.

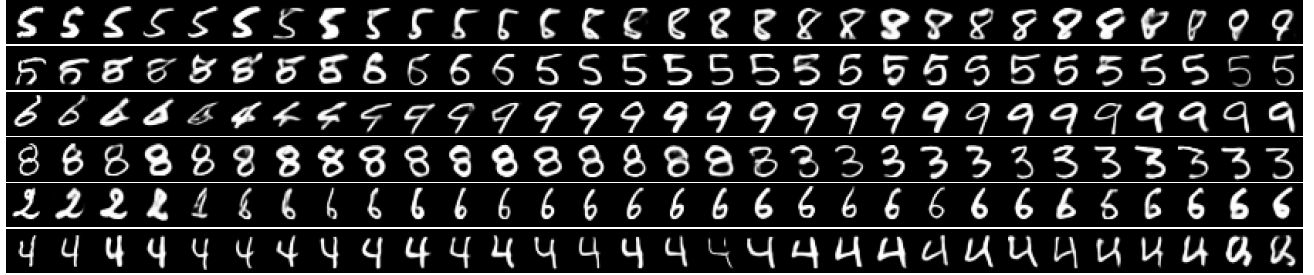


Figure 6. Cyclic generation starting from a training data point. Samples generated from an Exemplar VAE starting from a training data point, and then reusing the generated data as exemplars for the next round of generation (left to right).

## C. Reconstruction vs. KL

Table 9 shows the value of KL and the reconstruction terms of ELBO, computed based on a single sample from the variational posterior, averaged across test set. These numbers show that not only the exemplar VAE improves the KL term, but also the reconstruction terms are comparable with the VampPrior.

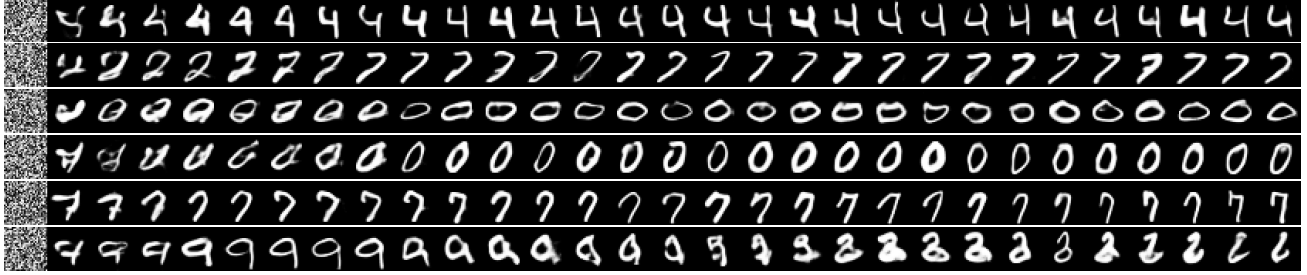


Figure 7. Cyclic generation starting from a noise input (left to right).

Model	Dynamic MNIST		Fashion MNIST		Omniglot	
	KL	Neg.Reconst.	KL	Neg. Reconst.	KL	Neg. Reconst.
VAE w/ Gaussian prior	25.54±0.12	63.06±0.11	18.38±0.11	213.21±0.18	32.97±0.2	82.3±0.21
VAE w/ VampPrior	25.14±0.16	<b>60.79</b> ±0.13	18.44±0.06	211.37±0.04	34.17±0.22	<b>79.49</b> ±0.18
Exemplar VAE	<b>24.82</b> ±0.22	61.00±0.13	<b>18.32</b> ±0.08	<b>211.10</b> ±0.1	<b>32.66</b> ±0.27	80.25±0.62
HVAE w/ Gaussian prior	26.80±0.13	59.80±0.11	19.08±0.05	211.18±0.14	<b>36.07</b> ±0.12	75.96±0.12
HVAE w/ VampPrior	26.69±0.1	<b>58.46</b> ±0.06	19.27±0.15	<b>210.04</b> ±0.2	38.39±0.16	<b>72.42</b> ±0.34
Exemplar HVAE	<b>26.41</b> ±0.17	58.48±0.16	<b>18.96</b> ±0.15	210.40±0.16	36.76±0.25	73.35±0.63
ConvHVAE w/ Gaussian prior	26.58±0.27	57.64±0.57	20.34±0.04	208.11±0.06	38.90±0.22	67.22±0.1
ConvHVAE w/ VampPrior	26.57±0.17	56.18±0.03	20.65±0.19	<b>206.64</b> ±0.15	38.95±0.17	<b>66.38</b> ±0.3
Exemplar ConvHVAE	<b>26.41</b> ±0.25	<b>56.14</b> ±0.27	<b>20.46</b> ±0.23	207.18±0.38	<b>37.48</b> ±0.37	66.62±0.32

Table 9. KL and reconstruction part of ELBO averaged over test set by a single sample from posterior.

## D. Experimental Details

### D.1. Architectures

All of the neural network architectures are based on the VampPrior of Tomczak & Welling (Tomczak & Welling, 2018), the implementation of which is available online<sup>1</sup>. We leave tuning the architecture of Exemplar VAEs to future work. To describe the network architectures, we follow the notation of LARS (Bauer & Mnih, 2018). Neural network layers used are either convolutional (denoted CNN) or fully-connected (denoted MLP), and the number of units are written inside a bracket separated by a dash (e.g., MLP[300-784] means a fully-connected layer with 300 input units and 784 output units). We use curly bracket to show concatenation.

Three different architectures are used in the experiments, described below.  $d_z$  refers to the dimensionality of the latent space.

#### a) VAE:

$$\begin{aligned} q_\phi(\mathbf{z} \mid \mathbf{x}) &= \mathcal{N}(\mathbf{z}; \mu_{\mathbf{z}}(\mathbf{x}), \Lambda_{\mathbf{z}}(\mathbf{x})) \\ p_\phi(\mathbf{x} \mid \mathbf{z}) &= \text{Bernoulli}(x, \mu_{\mathbf{x}}(\mathbf{z})) \end{aligned}$$

$$\begin{aligned} \text{Encoder}_{\mathbf{z}}(\mathbf{x}) &= \text{MLP} [784 - 300 - 300] \\ \log \Lambda_{\mathbf{z}}^2(\mathbf{x}) &= \text{MLP} [\text{Encoder}_{\mathbf{z}}(\mathbf{x}) - d_{\mathbf{z}}] \\ \mu_{\mathbf{z}}(\mathbf{x}) &= \text{MLP} [\text{Encoder}_{\mathbf{z}}(\mathbf{x}) - d_{\mathbf{z}}] \\ \mu_{\mathbf{x}}(\mathbf{z}) &= \text{MLP} [d_{\mathbf{z}} - 300 - 300 - 784] \end{aligned}$$

<sup>1</sup>[https://github.com/jmtomczak/vae\\_vampprior](https://github.com/jmtomczak/vae_vampprior)

b) **HVAE**:

$$\begin{aligned}
 q_\phi(\mathbf{z}_2 \mid \mathbf{x}) &= \mathcal{N}(\mathbf{z}_2; \mu_{\mathbf{z}_2}(\mathbf{x}), \Lambda_{\mathbf{z}_2}(\mathbf{x})) \\
 q_\phi(\mathbf{z}_1 \mid \mathbf{x}, \mathbf{z}_2) &= \mathcal{N}(\mathbf{z}_1; \mu_{\mathbf{z}_1}(\mathbf{x}, \mathbf{z}_2), \Lambda_{\mathbf{z}_1}(\mathbf{x}, \mathbf{z}_2)) \\
 p_\phi(\mathbf{z}_1 \mid \mathbf{z}_2) &= \mathcal{N}(\mathbf{z}_1; \hat{\mu}_{\mathbf{z}_1}(\mathbf{z}_2), \hat{\Lambda}_{\mathbf{z}_1}(\mathbf{z}_2)) \\
 p_\phi(\mathbf{x} \mid \mathbf{z}_1, \mathbf{z}_2) &= \text{Bernoulli}(\mathbf{x}, \mu_{\mathbf{x}}(\mathbf{z}_1, \mathbf{z}_2))
 \end{aligned}$$

$$\begin{aligned}
 \text{Encoder}_{\mathbf{z}_2}(\mathbf{x}) &= \text{MLP}[784 - 300 - 300] \\
 \log \Lambda_{\mathbf{z}_2}^2(\mathbf{x}) &= \text{MLP}[\text{Encoder}_{\mathbf{z}_2}(\mathbf{x}) - d_{\mathbf{z}_2}] \\
 \mu_{\mathbf{z}_2}(\mathbf{x}) &= \text{MLP}[\text{Encoder}_{\mathbf{z}_2}(\mathbf{x}) - d_{\mathbf{z}_2}] \\
 \text{Encoder}_{\mathbf{z}_1}(\mathbf{x}, \mathbf{z}_2) &= \text{MLP}[\{\text{MLP}[d_{\mathbf{z}_2} - 300], \text{MLP}[784 - 300]\} - 300] \\
 \log \Lambda_{\mathbf{z}_1}^2(\mathbf{x}, \mathbf{z}_2) &= \text{MLP}[\text{Encoder}_{\mathbf{z}_1}(\mathbf{x}, \mathbf{z}_2) - d_{\mathbf{z}_1}] \\
 \mu_{\mathbf{z}_1}(\mathbf{x}, \mathbf{z}_2) &= \text{MLP}[\text{Encoder}_{\mathbf{z}_1}(\mathbf{x}, \mathbf{z}_2) - d_{\mathbf{z}_1}] \\
 \text{Decoder}_{\mathbf{z}_1}(\mathbf{z}_2) &= \text{MLP}[d_{\mathbf{z}_2} - 300 - 300] \\
 \log \hat{\Lambda}_{\mathbf{z}_1}^2(\mathbf{z}_2) &= \text{MLP}[\text{Decoder}_{\mathbf{z}_1}(\mathbf{z}_2) - d_{\mathbf{z}_1}] \\
 \hat{\mu}_{\mathbf{z}_1}(\mathbf{z}_2) &= \text{MLP}[\text{Decoder}_{\mathbf{z}_1}(\mathbf{z}_2) - d_{\mathbf{z}_1}] \\
 \mu_{\mathbf{x}}(\mathbf{z}_1, \mathbf{z}_2) &= \text{MLP}[\{\text{MLP}[d_{\mathbf{z}_1} - 300], \text{MLP}[d_{\mathbf{z}_2} - 300]\} - 300 - 784]
 \end{aligned}$$

c) **ConvHVAE**: The generative and variational posterior distributions are identical to HVAE.

$$\begin{aligned}
 \text{Encoder}_{\mathbf{z}_2}(\mathbf{x}) &= \text{CNN}[28 \times 28 \times 1 - 32 \times 32 \times 32 - 12 \times 12 \times 32 - 12 \times 12 \times 64 - 7 \times 7 \times 64 - 7 \times 7 \times 6] \\
 \log \Lambda_{\mathbf{z}_2}^2(\mathbf{x}) &= \text{MLP}[\text{Encoder}_{\mathbf{z}_2}(\mathbf{x}) - d_{\mathbf{z}_2}] \\
 \mu_{\mathbf{z}_2}(\mathbf{x}) &= \text{MLP}[\text{Encoder}_{\mathbf{z}_2}(\mathbf{x}) - d_{\mathbf{z}_2}] \\
 \text{ConvEncoder}_{\mathbf{z}_1}(\mathbf{x}) &= \text{CNN}[28 \times 28 \times 1 - 32 \times 32 \times 32 - 12 \times 12 \times 32 - 12 \times 12 \times 64 - 7 \times 7 \times 64 - 7 \times 7 \times 6] \\
 \text{Encoder}_{\mathbf{z}_1}(\mathbf{x}, \mathbf{z}_2) &= \text{MLP}[\{\text{MLP}[d_{\mathbf{z}_2} - 7 \times 7 \times 6], \text{ConvEncoder}_{\mathbf{z}_1}(\mathbf{x})\} - 300] \\
 \log \Lambda_{\mathbf{z}_1}^2(\mathbf{x}, \mathbf{z}_2) &= \text{MLP}[\text{Encoder}_{\mathbf{z}_1}(\mathbf{x}, \mathbf{z}_2) - d_{\mathbf{z}_1}] \\
 \mu_{\mathbf{z}_1}(\mathbf{x}, \mathbf{z}_2) &= \text{MLP}[\text{Encoder}_{\mathbf{z}_1}(\mathbf{x}, \mathbf{z}_2) - d_{\mathbf{z}_1}] \\
 \text{Decoder}_{\mathbf{z}_1}(\mathbf{z}_2) &= \text{MLP}[d_{\mathbf{z}_2} - 300 - 300] \\
 \log \hat{\Lambda}_{\mathbf{z}_1}^2(\mathbf{z}_2) &= \text{MLP}[\text{Decoder}_{\mathbf{z}_1}(\mathbf{z}_2) - d_{\mathbf{z}_1}] \\
 \hat{\mu}_{\mathbf{z}_1}(\mathbf{z}_2) &= \text{MLP}[\text{Decoder}_{\mathbf{z}_1}(\mathbf{z}_2) - d_{\mathbf{z}_1}] \\
 \text{MLPDecoder}_{\mathbf{x}}(\mathbf{z}_1, \mathbf{z}_2) &= \text{MLP}[\{\text{MLP}[d_{\mathbf{z}_1} - 300], \text{MLP}[d_{\mathbf{z}_2} - 300]\} - 784] \\
 \text{ConvDecoder}_{\mathbf{x}} &= \text{CNN}[28 \times 28 \times 64 - 28 \times 28 \times 1] \\
 \mu_{\mathbf{x}}(\mathbf{z}_1, \mathbf{z}_2) &= [\text{MLPDecoder}_{\mathbf{x}}(\mathbf{z}_1, \mathbf{z}_2) - \text{ConvDecoder}_{\mathbf{x}}]
 \end{aligned}$$

As the activation function, the gating mechanism of (Dauphin et al., 2017) is used throughout. So for each layer we have two parallel branches where the sigmoid of one branch is multiplied by the output of the other branch. In ConvHVAE the kernel size of the first layer of  $\text{Encoder}_{\mathbf{z}_2}(\mathbf{x})$  is 7 and the third layer used kernel size of 5. The last layer of  $\text{ConvDecoder}_{\mathbf{x}}$  used kernel size of 1 and all the other layers used  $3 \times 3$  kernels.

## D.2. Hyper-parameters

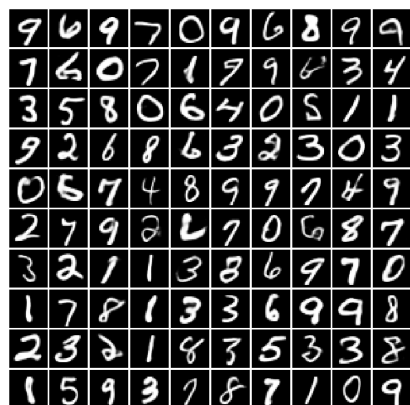
We use Graident Normalized Adam (Yu et al., 2017b) with Learning rate of  $5e - 4$  and minibatch size of 100 for all of the datasets. We dynamically binarize each training data, but we do not binarize the exemplars that serve as the prior. We utilize early stopping for training VAEs, where we stopped the training if for 50 consecutive epochs the validation ELBO does not improve. In all of the experiments, we use 40 dimensional latent spaces both for hierarchical and non-hierarchical architectures. To limit the computation costs of ConvHVAE, we considered kNN based on euclidean distance in the latent space, where  $k$  set to 10. The number of exemplars set to the half of the training data except in the ablation study section.

## E. Misclassified MNIST Digits

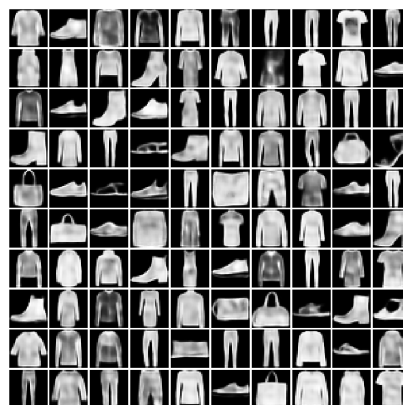


Figure 8. Misclassified images from MNIST test set for a two layer MLP trained with Exemplar VAE augmentation.

## F. Additional Samples



MNIST



Fashion MNIST



Omniglot

Figure 9. Random samples generated by three Exemplar VAEs trained on MNIST, Fashion MNIST, and Omniglot.

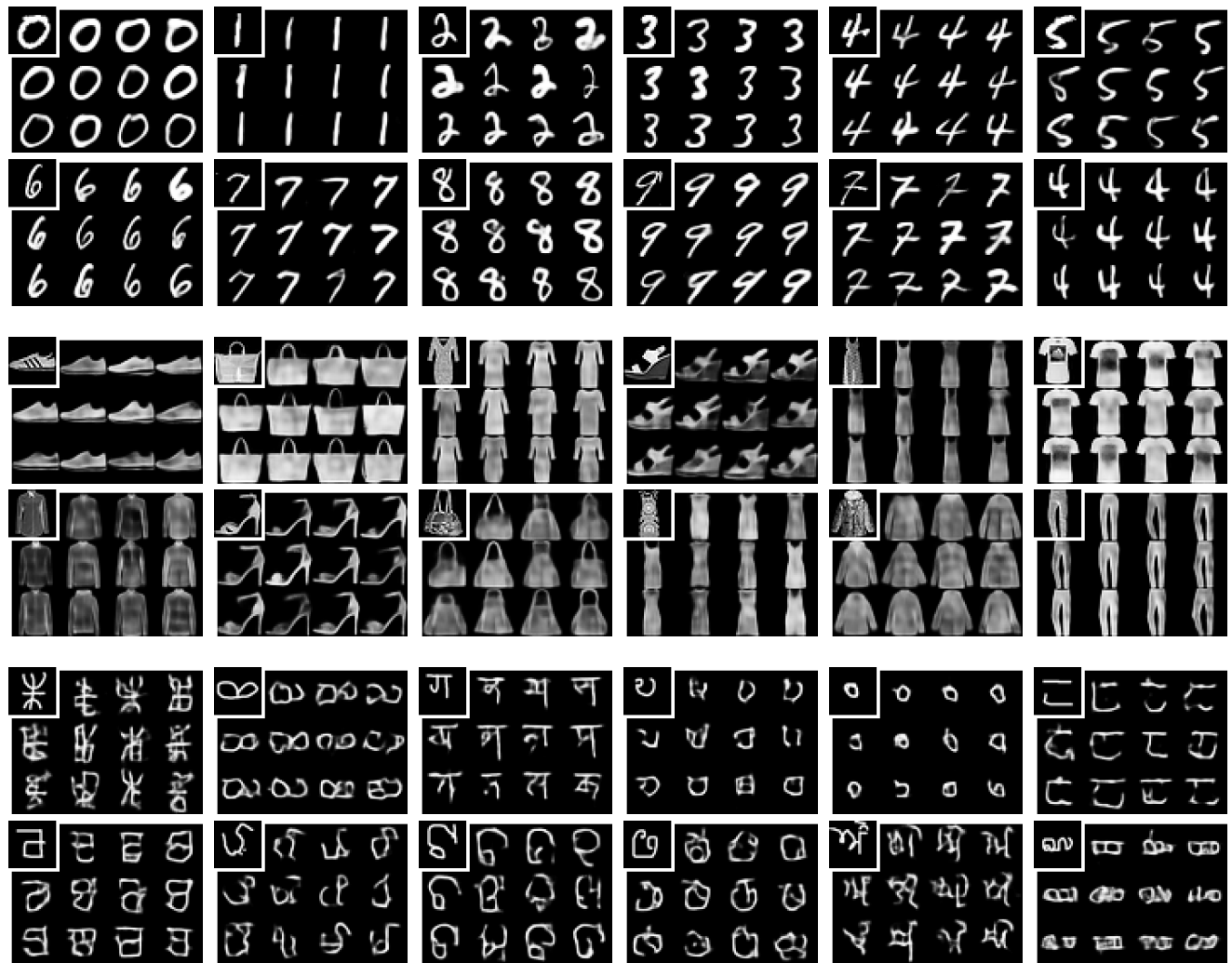


Figure 10. Given the input exemplar on the top left of each plate, 11 conditional Exemplar VAE samples are generated and shown.